Chapter 11

Anisotropic Velocity Analysis

Tying well tops to seismic reflections requires detailed discussion of time-to-depth and depth-to-time conversion, as well as migration to true depth. Historically, tying wells to a seismic migration was called *depthing* and usually converted only a few horizons to depth. This depthing process was almost solely focused on ultimately providing an accurate conversion of an interpreted migrated time map to depth in such a manner that the horizon depth in all wells within the mapped area were matched as precisely as possible. This process was not concerned with producing depth volumes containing all horizons of interest; it was only concerned with matching well tops. Accomplishing this feat required that all well tops of interest be tied to the corresponding seismic time image with precise accuracy. When necessary, well velocities were modified to fit the observed discrepancies, and, after much trial and error, a suitable velocity $v_0(x,y)$ map for depth conversion of the given horizon was produced. The underlying assumption in all of this was that the time migrated volume was as accurate as necessary, and well discrepancies were just a function of measurement error. It is now known that the truth is not so simple. The reason we had to tie the seismic data to the well was that the migration was performed with no consideration for anisotropic wave propagation.

The single most important parameter associated with anisotropic migration is the 3D Earth model. Note that it is not just the simple velocity model normally used in prestack time (RMS) or prestack depth (INTERVAL) migrations. This model has at least three, and up to five, interrelated parameters.

The best known elements of this five-member set are the sound speed, determined through iterative migration velocity analysis, and the well-based or *true* depth velocity field. Frequently, these two fields are considered to be independent and totally unrelated, but the theoretical facts are completely out of phase with this concept. In fact, these two fields are the most important aspects of what is required to produce migrated images that exactly tie the wells.

While the two velocity fields are necessary, they are not sufficient to complete the process. In addition, we must also determine how these two fields are related to accurately image the recorded data at the precise subsurface location from which they were reflected. In the sections on velocity analysis and velocity model building, we develop and discuss the data, workflow, tools, and concepts necessary to construct the entire Earth model.

There is no doubt that there are still many geophysicists who believe that true depth imaging is not possible and will never be possible. What we argue is that all of these approaches have their place, but in the final analysis, the optimum approach must incorporate the full anisotropic model to achieve true depth conversion at all dips. Integration of all available data is key and must be performed accurately for this to produce high quality results.

Anisotropic Earth Models

Estimating an anisotropic Earth model is not easy. In the best case, the seismic data on which anisotropic parameters are based contain the necessary information to facilitate accurate velocity estimation. However, since this is not likely to be the case, we must make do with what we have.

Figure 11-1(a) is a graphic of why normal seismic velocity analysis does not generally provide an Earth model suitable for accurate depth imaging. The blue ray fronts indicate that the lateral velocity is faster than the vertical velocity shown in magenta. Semblance analysis tends to produce estimates of the lateral velocity variation and not the vertical variation. That is, in the specified Earth model used to compute the ray fronts, the magenta ray fronts are not present, so when velocities are estimated, the resulting interval velocity will be more proportional to the faster lateral sound speed. So long as we use a short spread analysis, as specified by Figure 11-1(b), our Earth model velocity field will be too fast. Nevertheless, it normally provides us with excellent images and a velocity field that can be used to estimate δ in conjunction with a suitable well field.

Figure 11-1. Anisotropic Ray Fronts and Short Spread Semblance Velocity Analysis

(a). Anisotropic ray fronts

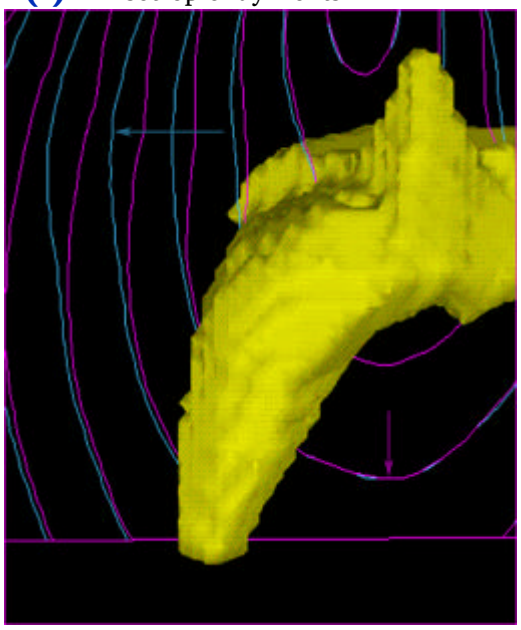

(b). Short spread semblance velocity analysis

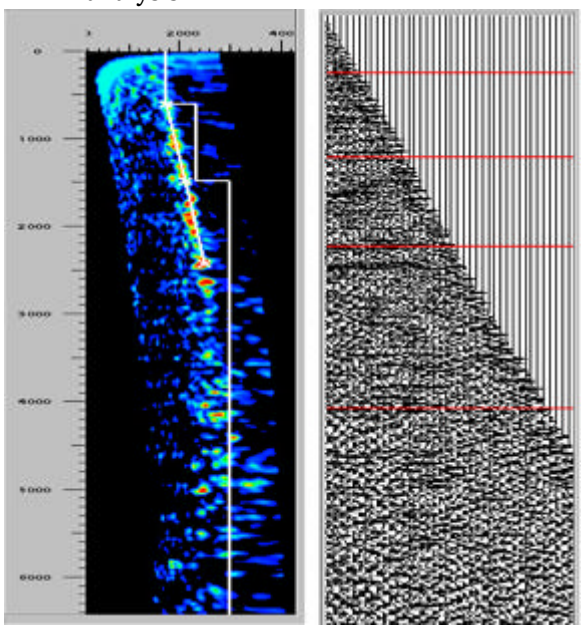

The Anisotropic Earth

Figure 11-2(a) shows conclusively that the Earth we know and love is definitely anisotropic. What we see in this figure is a comparison between an isotropic and an anisotropic migration of a small piece of a seismic section and well as a direct comparison to to data from a VSP-CDP transform section. The 3D vertical seismic profiles (VSPs), as shown in Figure 11-2(b), could provide virtually all of the additional anisotropic parameters in cone relative to the central well location. As shown in Figure 11-3, VSPs provide a superb approach for tying surface seismic data to reflecting horizons and are perhaps one of the best methods for both recognizing and proving the existence of anisotropy in real rocks. Unfortunately, VSPs provide information about anisotropy only at a relatively sparse set of well locations. To construct full wide area 3D anisotropic modes necessitates that we find methods for using recorded seismic data to extend the estimation area.

Figure 11-2. Vertical Seismic Profiles and Their Use in Depthing

(a). VSP-CDP transform, anisotropic versus isotropic migration

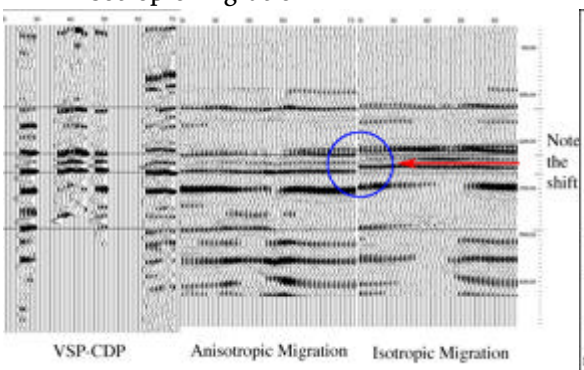

(b). 3D VSP after imaging

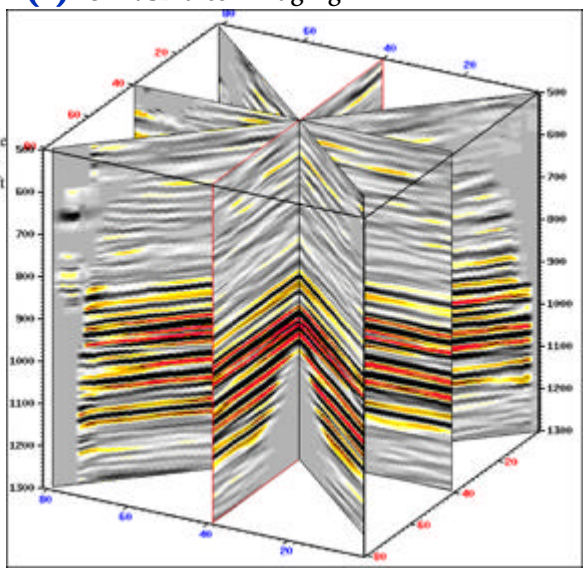

Figure 11-3. VSP tying surface data to reflecting horizons

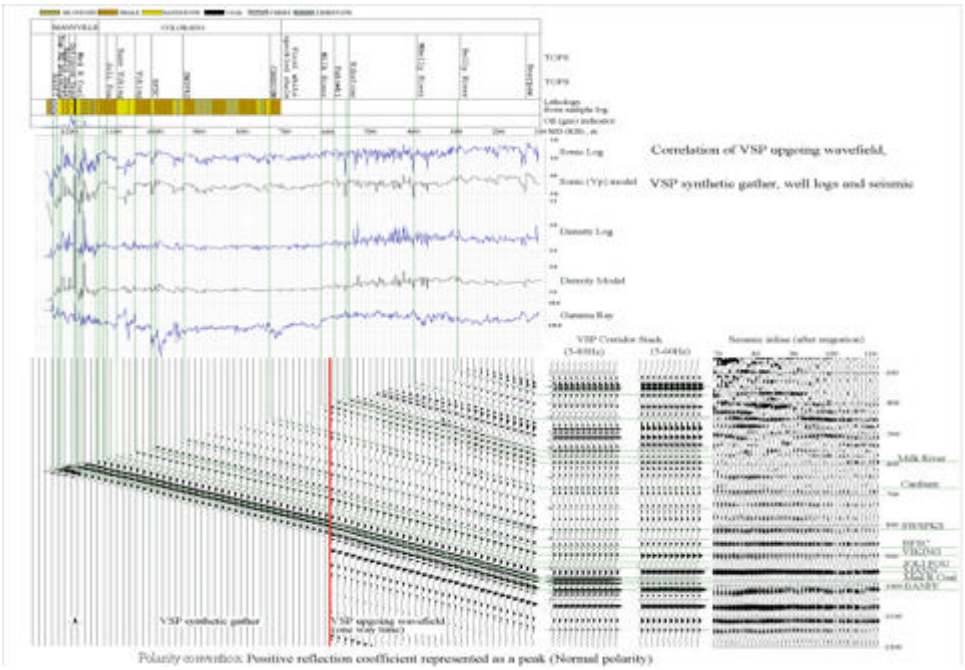

Anisotropic Normal Moveout

Today we know that the Earth is mostly anisotropic. When we estimate velocities in the isotropic case, we are trading offset information for what we think is vertical velocity. In an anisotropic world this necessarily implies that we are estimating angle dependent sound speeds and as a result we should not expect to produce images that match our wells in any form or fashion. We also should not expect our traditional isotropic velocity analysis to completely flatten common-midpoint gathers. Figure Figure 11-4 demonstrates what happens when we do. Here we see the so-called *hockey sticks* so prevalent in anisotropic media. In the past these patterns were usually muted off so as to improve overall image quality. What we really should have done was to try to figure out how to use this information to produce more accurate subsurface images.

Figure 11-4. After Leon Thomsen DSC 2002. Typical *hockey stick* character after application of *NMO* using the usual stacking velocity equation without the anisotripic term.

As we saw in the chapter on modeling, the moveout in a VTI medium is specified by the anisotropic normal moveout equation, Equation 2-26, which has been at least partially empirically corrected in Equation 11-1.

(11-1)
$$t^2(h) = t_0^2 + \frac{h^2}{v_{nmo}^2} - \frac{(v_{hor}^2 - v_{nmo}^2)h^4}{v_{nmo}^2(t_0^2 v_{nmo}^4 + 1.2 v_{hor}^2 h^2)}$$

Several important observations can be made concerning this equation. The first two terms are identical to the equation we currently use for both time and depth velocity estimation. Thus, we are already familiar with how they work and how we can use them to advantage. Because the difference between v_{nmo} and v_{hor} is usually small they are also the dominant terms when the half offset h is relative short.

At first glance this suggests that we can perform an anisotropic velocity analysis as a two step process. The first step ignores v_{hor} and just estimates v_{nmo}. Once v_{nmo} is available a second pass through the data provides estimates for v_{hor}. As we will see we can also perform a 3D velocity analysis at each vector midpoint for a simultaneous estimate of these important parameters.

Although known to be somewhat less statistically stable than Equation 11-1, Equation 11-2 relates the offset dependent traveltime $t^2(h)$ to v_{nmo} and the so-called η parameter defined by ε and δ as Equation 11-3.

(11-2) $$t^2(h) = t_0^2 + \frac{h^2}{v_{nmo}^2} - \frac{2\eta h^4}{v_{nmo}^2[t_0^2 v_{nmo}^2 + (1+2\eta)h^2]}$$

(11-3) $$\eta = \frac{\varepsilon - \delta}{\sqrt{1+2\delta}}$$

As was the case for Equation 11-1, once v_{nmo} has been determined, η can be estimated through a semblance-based process similar to the familiar stacking velocity analysis used to find v_{nmo}.

These two formulas can also be used in what you might call a simultaneous inversion for either v_{nmo} and v_{hor}, or for v_{nmo} and η. What is different is that the semblance panels are 3D volumes of two of the parameters and time.

Figure 11-5 is after Tsvankin (2001), where (a) shows an anisotropic arrival curve from a VTI media, and (b) shows the contours of a semblance analysis at 1.0 seconds; in this case, an estimate of $v_{hor} = 2.3$ and $v_{nmo} = 2.0$ is quite realistic. Part (c) shows that a value of $\eta \approx .16$ would not be completely inappropriate.

Figure 11-5. Estimating Vnmo and Vhor

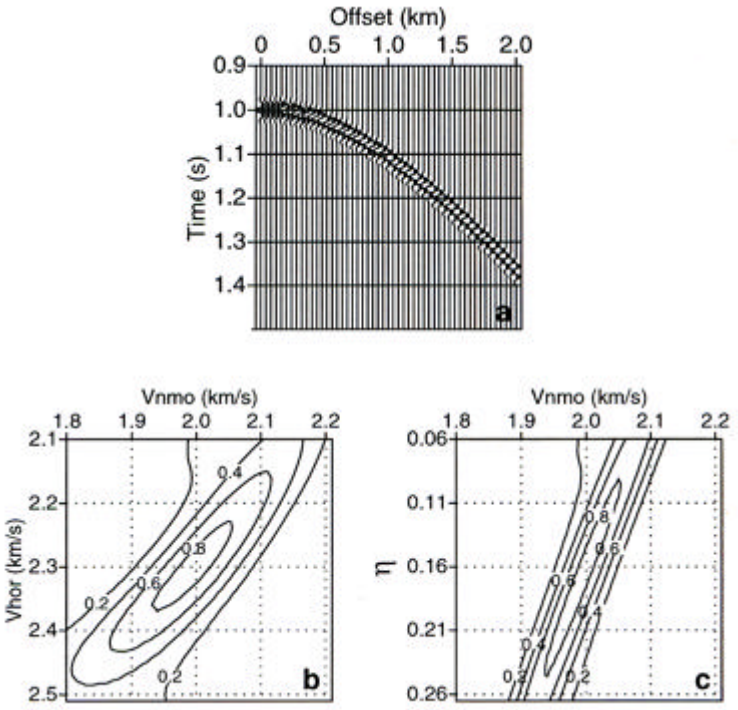

Figure Figure 11-5 provides a simple glimpse of the *NMO* based inversion process. Part (a) shows a single arrival from a reflector embedded in an anisotropic medium. The zero-offset time t_0 of this reflector is 1 second. In this case, the model *NMO* velocity is 2.0 meters/second, the model horizontal velocity, v_{hor}, is 2.3 kilometers/second and the η of the model is 0.16. Part (b) shows a slice at 1 second through a 3D $v_{nmo} - v_{hor}$ velocity analysis of the data in part (a). Clearly, values of $v_{nmo} = 2.0$ and $v_{hor} = 2.3$ kilometers per second are reasonable choices. Part (c) shows the similar panel for v_{nmo} and η. Since v_{nmo} is known from part (b) choosing $\eta = 0.16$ would not be out of line.

Following the process described above yields three parameters, v_{nmo}, v_{hor} and η. Because η is defined in terms of ε and δ, we must find some process which allows us to find either δ or ε. Once determined, we will have achieved the first step in developing a model that describes compressional wave propagation in an anisotropic medium. A quick review of the section on Thomsen parameters reveals that

(11-4)
$$\varepsilon \approx \frac{v_{hor}}{v_{P0}} - 1$$

Thus, we need a process to determine v_{P0} so we can estimate δ algebraically. To do so, we measure vertical velocities in a well. Although the measurements are at higher frequencies then seismic sound speeds, these can always be modified as the need arises. This means that we need a process for constructing a vertical well field. Once we have that, we can construct our VTI Earth model from our *NMO* based estimates, with the exception of γ.

Depthing

Geophysical approaches to finding vertical velocity fields abound. Some of the earliest were called *depthing*, or, perhaps more precisely, *depth conversion*. Depth conversion typically begins with a careful analysis of the wells of interest.

Figure 11-6(a) shows how the overburden above the potential reservoir is separated into different velocity units. Starting at the surface, we model the velocity behavior in layer 1 and create a depth map for horizon 1. We then model the velocity in layer 2 and hang the depth conversion from the depth horizon we already have for horizon 1. We repeat the process for each layer until we reach the maximum depth desired.

Figure 11-6. Analyzing wells for unitized velocities

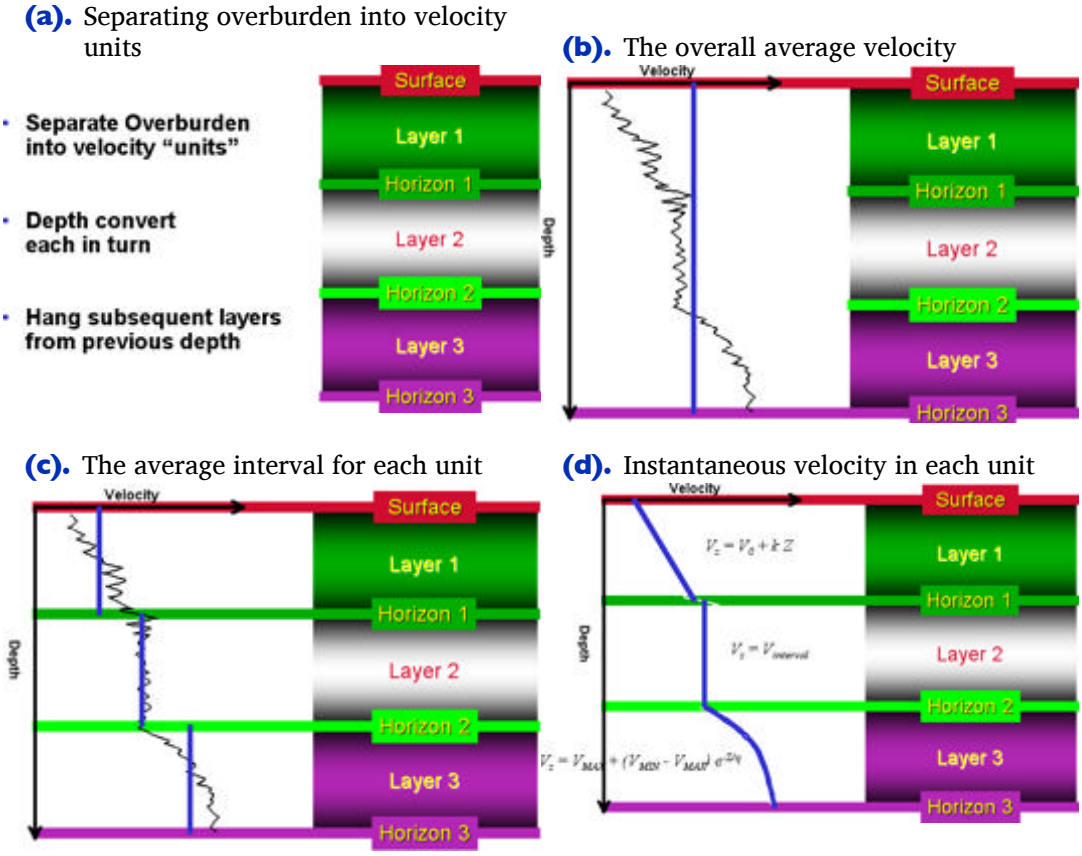

Figure 11-6 shows the typical approach to analyzing wells to determine a well or depthing velocity structure. The graphic in (a) of this figure presents the standard process. The well is separated into overburden units or well tops of horizons of interest. Each of these units can then be converted to depth. Analysis of each such unit can be simple, as indicated in Figure 11-6(b), or more complicated as indicated in (c) and (d). The more accurate approach is clearly represented by Figure 11-6(d).

Depending on the complexity and strength of the velocity variation within the well, we can minimize the number of depth units. Figure 11-6(b) shows the simplest technique using a single average velocity. We ignore the layering just described, and compute an average velocity from the surface to the target horizon. This has the advantage of being simple and quick to implement, but has the disadvantage that, since the behavior of the subsurface is not fully modeled, our confidence in the predictions may be reduced. This is a good domain for viewing stacking velocities, because they have seen all of the overburden anyway.

Moving to a more sophisticated approach in Figure 11-6(c), we look at interval velocity. Here, we assign a constant velocity to each layer. This velocity may vary spatially from well to well. We can model this by cross plotting interval velocity versus midpoint depth, for example, or we can contour the well interval velocities, perhaps geostatistically using our seismic processing velocities as a guide.

An even more sophisticated approach, as shown in Figure 11-6(d), is the use of instantaneous velocity functions. Here we are modeling the detailed velocity variation with depth on a layer-by-layer basis. The most commonly used relationship is the linear increase of velocity with depth (the V0Kz method), although modern software packages can handle any function, as shown in the third layer. Any of the parameters in these equations can be represented by grids, thus allowing full flexibility.

Constructing complex horizon-based models can be quite difficult. Figure 11-7 illustrates several requirements for different geological settings. What is important is to recognize that in a horizon-based model building exercise, we must interpret many more horizons than is usually necessary for exploration purposes. Moreover, many of the additional horizons have zero prospectivity and, consequently, are of little interest to interpreters, although these layers can be extremely important for depth imaging.

Figure 11-7. Complex model construction

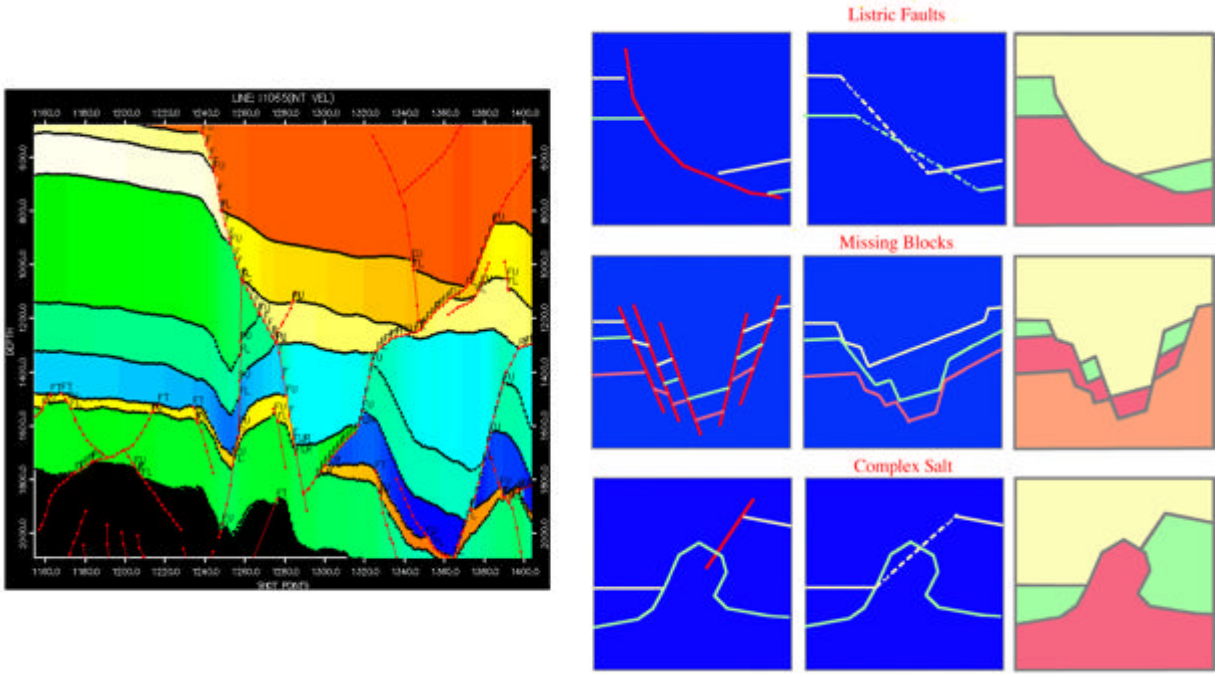

Horizontal velocity trends are thought to be linked with vertical velocity trends. Thus, using trends from the prestack depth migration velocity analysis can be used to statistically interpolate sparse well data sets. Figure 11-8 is an example velocity slice from a seismically derived Earth model. It could serve to define trends for extrapolating sparse wells to construct a detailed well field.

Figure 11-8. Seismic derived velocity slice.

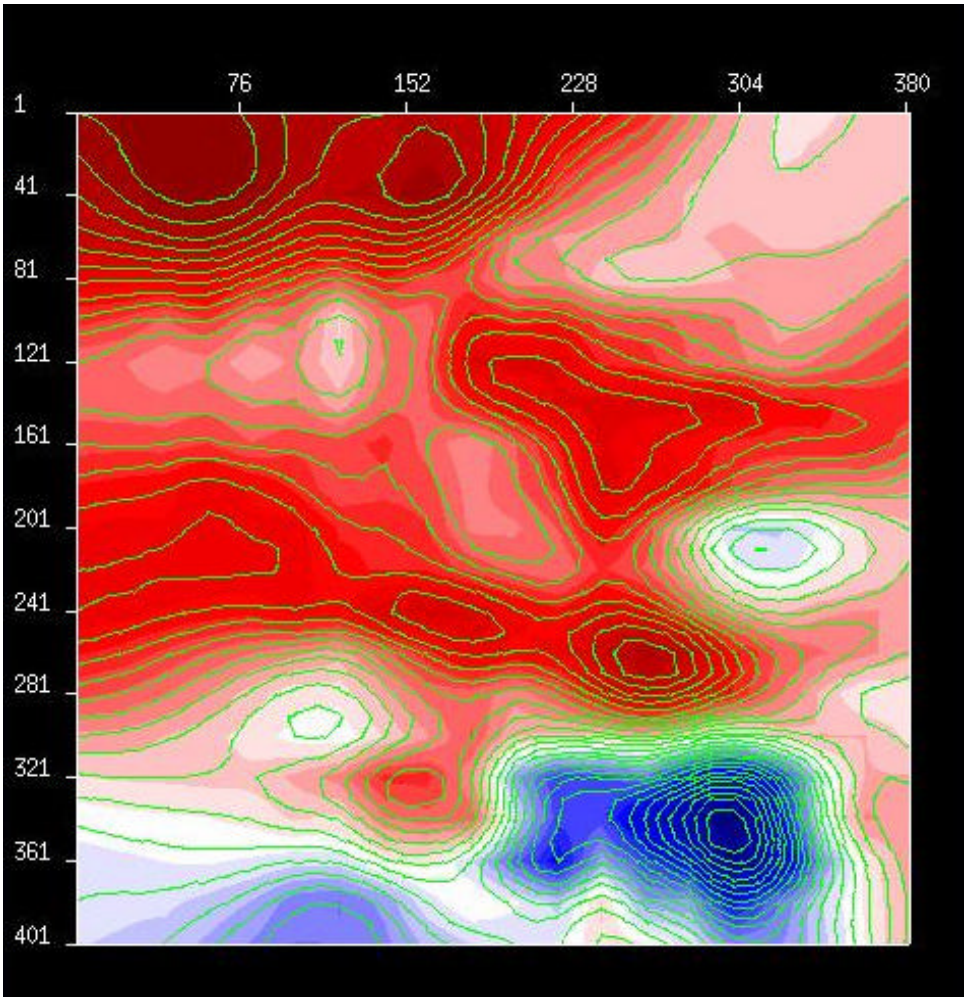

Horizons, like those in Figure 11-9(a), can be used to guide the interpolation process in a horizon consistent in a lap or off lap manner. If we decide that the subsurface geology follows the structure defined by the given horizons, a suitable projection of this estimated velocity functions on to a grid of locations defined by the user will produce a structure tracking velocity field.

Figure 11-9. Single Well Velocity Field

(a). A multiple horizon model

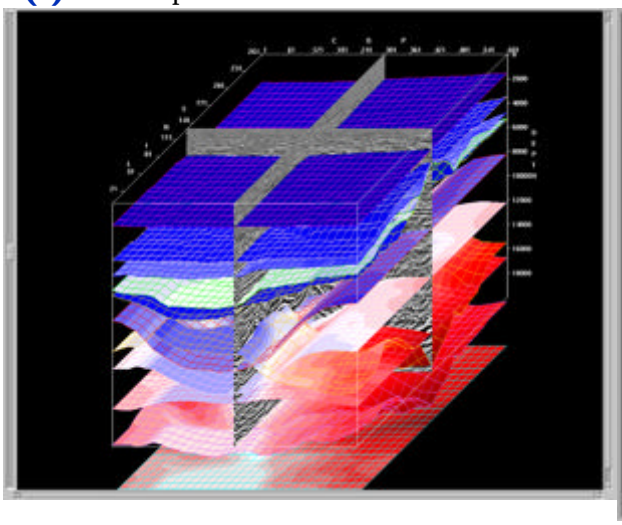

(b). A single well at the indicated location

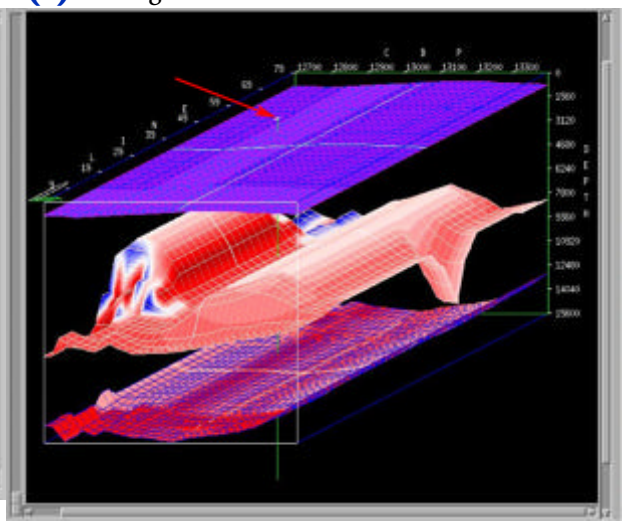

(c). Projected horizon tracking wells

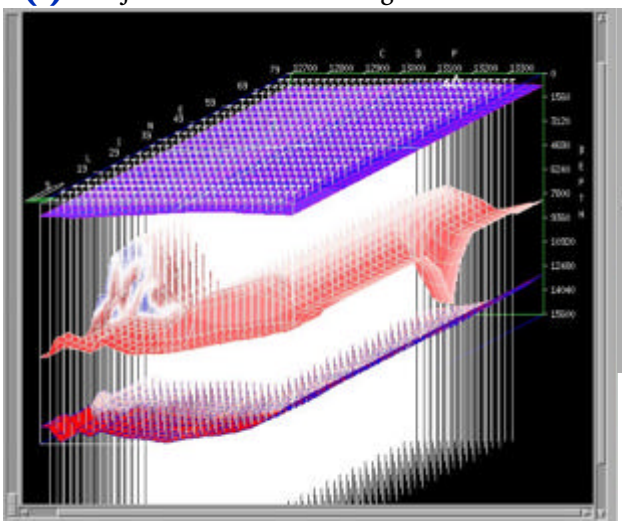

(d). A slice through the constructed model

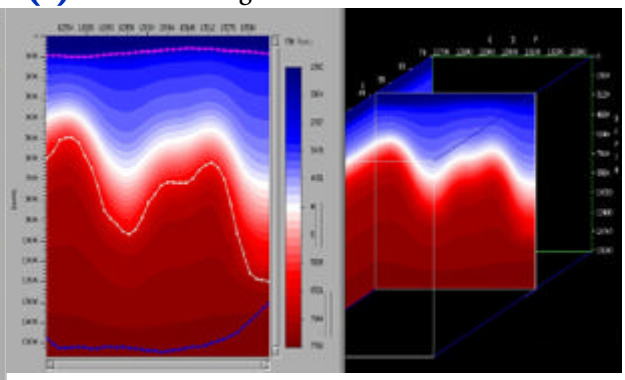

(e). Extracted RMS with interval velocity overlay

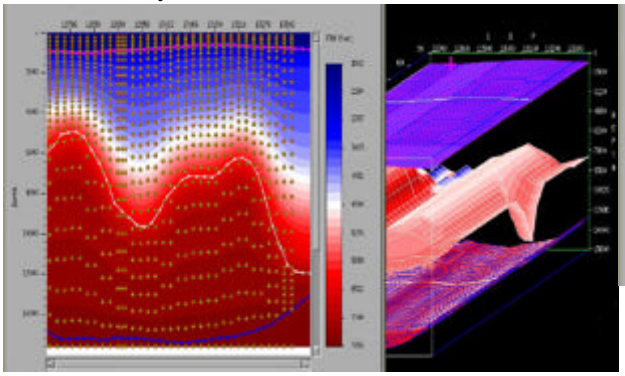

(f). Final Well field

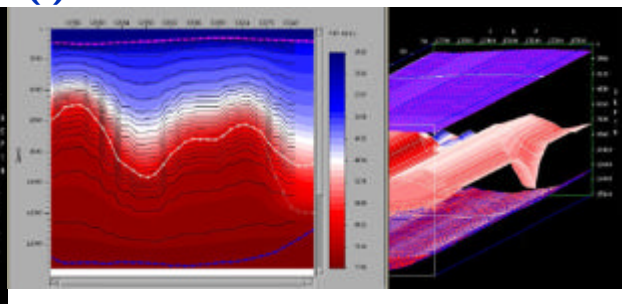

In Figure 11-9(b), a single well, at the location indicated by the arrow, is interactively projected into the three-dimensional grid. After projection, we have logs at an evenly sampled grid of surface locations, Figure 11-9(c). In this case, projection was based on shrinking and stretching the single input function to track the given horizons.

Figure 11-9(d) is a slice through the projected well field, while Figure (e) shows RMS velocities calculated from the well field. In a sense, this process reverses the usual process of estimating interval from RMS velocities. Figure (f) is a contoured version of (d) showing how the actual projection was performed.

A VTI example

Here we present an example of what one might expect from the analysis process discussed above. Figure 11-10 shows a vertical velocity (v_{P0}) field in (a) and a v_{nmo} field in (b). Because it is so similar to the vertical field the horizontal field v_{hor} is not shown. What we know from the previous analysis is that

(11-5) $$\varepsilon \approx \frac{v_{hor}}{v_{P0}} - 1$$

In this case, the ε volume is shown in Figure 11-12(b). Given Equation 11-6, we can easily solve for δ, thereby producing a complete three-dimensional volume. The result is shown in Figure 11-12(b).

(11-6) $$\eta = \frac{\varepsilon - \delta}{\sqrt{1 + 2\delta}}$$

Figure 11-10. Well and NMO Velocity Volume

(a). Estimated well velocity field

(b). Estimated short-spread MVA NMO velocity volume

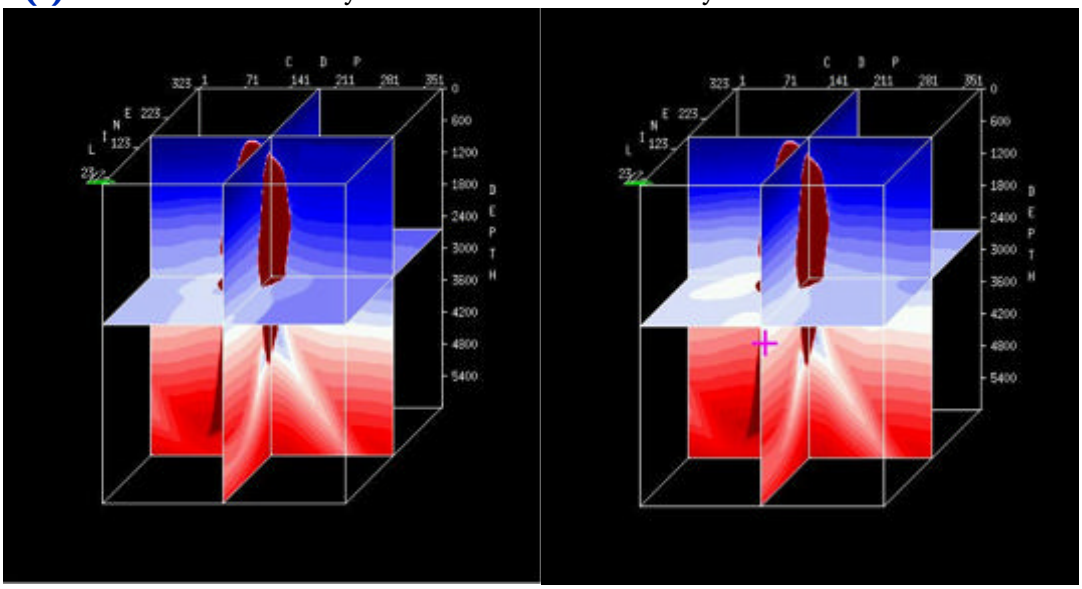

Figure 11-11. The η volume as estimated along with the v_{nmo} volume using Equation 11-2.

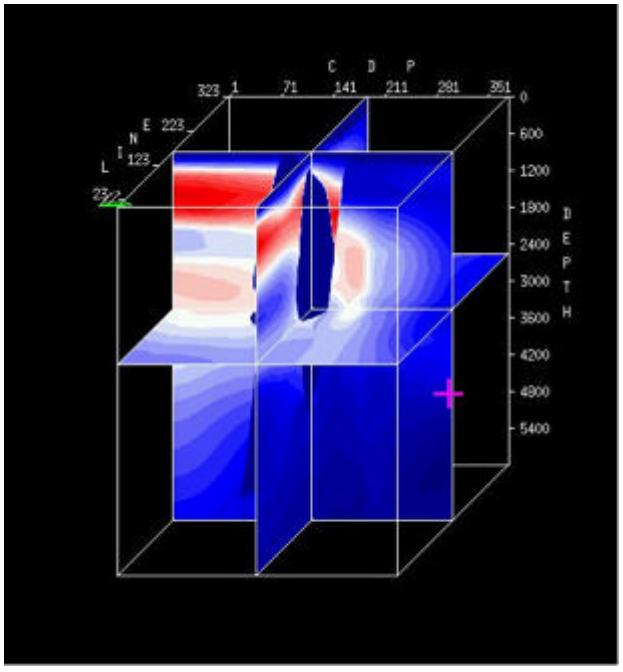

Figure 11-12. ε **and** η **volumes**

(a). The estimated ε volume.

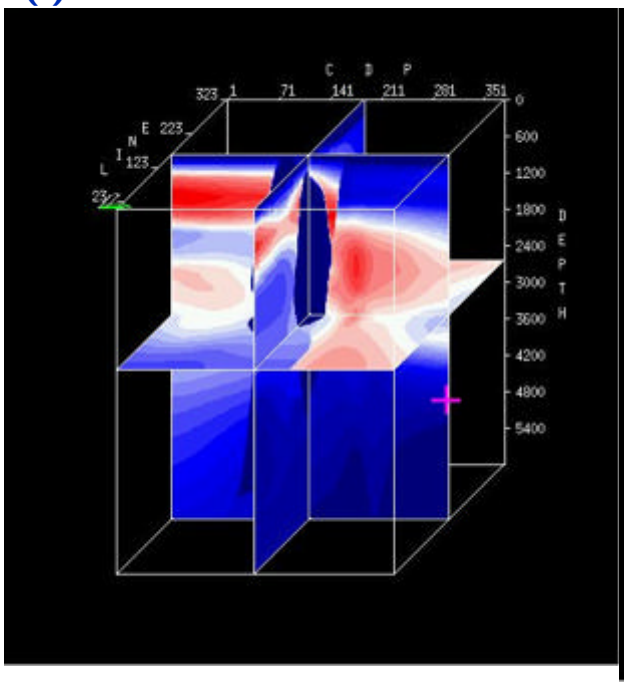

(b). The estimated δ volume.